Eur Biophys J (2008) 37:521–527
DOI 10.1007/s00249-007-0222-7

BIOPHYSICS LETTER

On the structures of filamentous bacteriophage Ff (fd, f1, M13)

S. K. Straus · W. R. P. Scott · M. F. Symmons · D. A. Marvin

Received: 1 August 2007 / Revised: 12 September 2007 / Accepted: 14 September 2007 / Published online: 18 October 2007

Abstract The filamentous bacteriophage (*Inovirus*) strain Ff (fd, f1, M13) is widely used in molecular biophysics as a simple model system. A low resolution molecular model of the fd protein coat has been reported, derived from iterative helical real space reconstruction of cryo-electron micrographs (cryoEM). This model is significantly different from the model previously derived from X-ray fibre diffraction and solid-state NMR. We show that the cryoEM model agrees neither with solid-state NMR data nor with X-ray fibre diffraction data of fd, and has some puzzling structural features, for instance nanometre holes through the protein coat. We refine the cryoEM model against the X-ray data, and find that the model after refinement closely approximates the model derived directly from X-ray fibre diffraction and solid-state NMR data. We suggest possible reasons for the differences between the models derived from cryoEM and X-ray diffraction.

Keywords α-Helix · Fibre diffraction · Solid-state NMR · Cryo-electron microscopy · Helical reconstruction

S. K. Straus · W. R. P. Scott
Department of Chemistry,
University of British Columbia,
Vancouver, BC, Canada V6T 1Z1

M. F. Symmons
Department of Pathology, University of Cambridge,
Cambridge CB2 1QP, UK

D. A. Marvin (✉)
Department of Biochemistry, University of Cambridge,
Cambridge CB2 1GA, UK
e-mail: d.a.marvin@bioc.cam.ac.uk

Abbreviations

CryoEM	Electron microscopy in vitreous ice
IHRSR	Iterative helical real space reconstruction
PDB	Protein data bank
rmsd	Root mean square deviation

Introduction

Biological macromolecules are flexible in solution. This is true of globular proteins, that may have active sites that change conformation as they act, and also of polymers that are semiflexible (wormlike) polyelectrolytes. However, with most experimental techniques that are used to determine structure, single molecules cannot be imaged due to low signal-to-noise ratios, and it is necessary to combine information from many molecules to create an image. A widely used method to combine information is to study an ordered array of identical molecules: a crystal of a globular protein or an ordered fibre of a polymer. Such experiments can give important insights into structure and function, but are sometimes criticized on the grounds that the molecules are not in their native solution state. Another approach is to computationally combine electron micrograph images from isolated single molecules. This method can give useful structural information without the phasing issues of X-ray diffraction, and it does not require preparation of an ordered array (a crystal or a fibre). Isolated molecules seen in an electron micrograph may be more like molecules in solution. This approach is especially useful for helical structures, because the internal helix symmetry gives additional constraints on the structure. The way to combine these images is clearer when internal structure is visible in the individual images, but a method has also been developed to combine images from electron microscopy in vitreous ice

(cryoEM) of helical structures when no internal structure is visible, namely the iterative helical real space reconstruction method (IHRSR), and this method has given important insights into many systems (Egelman 2000, 2007). Even for this method it is assumed that all images to be combined represent molecules that are in one, or a few, conformations, so the solution is both a space average and a time average of the true structures.

Filamentous bacteriophages are about 60 Å in diameter and 1–2 μm long (depending on the strain). Their protein coat is a helical shell of several thousand ~50-residue identical major coat protein subunits protecting a DNA core, with a few minor proteins capping the two ends. The phages are interesting model systems in structural biology, in part because of their unusual mechanism of assembly. This includes displacement of intracellular replication-assembly proteins from the phage DNA by the membrane-spanning coat proteins as the nascent phage is extruded through the bacterial plasma membrane into an ordered helical array. The physiology and genetics of filamentous bacteriophages in the Ff group, strains fd, f1 and M13, have been studied in most detail (reviewed by Marvin 1998; Webster 2001; Russel and Model 2006). However, the Pf1 strain of phage gives better X-ray fibre diffraction patterns than Ff. The architecture of Pf1 was determined initially by direct interpretation of the positions of strong intensity on the X-ray patterns, which showed that the major coat protein subunit is largely α-helical, with the axis of the helix tilted at a small angle to the axis of the phage and forming an overlapping interdigitated helical array of protein subunits (Marvin et al. 1974a; Marvin and Wachtel 1976). Heavy atom derivatives were used to resolve questions about the helix symmetry of Pf1 (Nave et al. 1981) and to calculate model-independent electron density maps using a maximum-entropy method (Bryan et al. 1983; Marvin et al. 1987). These electron density maps resolved the question of the hand of the virus helix, and were also used as the starting point for simulated annealing refinement of a molecular model with respect to quantitative X-ray data (Gonzalez et al. 1995). Further refinement led to the suggestion that the helix asymmetric unit in the higher-temperature form of Pf1 was a "group of three" polypeptide chains having slightly different orientations, rather than a single polypeptide chain (Welsh et al. 2000). Challenges to this suggestion based on solid-state NMR data (Thiriot et al. 2004) and magic-angle spinning unaligned NMR data (Goldbourt et al. 2007) were based on the deposited coordinates for the "group of three" polypeptide chains, in which there are slight differences not only in the orientations of the three subunits, but also in their conformation (because of the refinement method). But Welsh et al. (2000) also reported that if the subunits in the "group of three" are replaced by subunits with identical conformation but still with slightly different orientations, the model still explains the X-ray data (Fig. 5c of Welsh et al. 2000). This model also explains the NMR data (unpublished calculations), so the "group of three" model is not ruled out. But for most purposes, the simple helix model is a good working approximation to the structure.

The same architecture, with similar subunit shape but slightly different symmetry, was found for the fd strain (Marvin et al. 1974b; Banner et al. 1981) and other genetically unrelated strains, suggesting a common geometric theme (Marvin 1990). Building molecular models to compare with the experimental data is an essential part of the structure analysis, since the diffraction data do not contain information at atomic resolution. Models of fd have been revised and extended as additional data became available, not only diffraction data but also chemical, spectroscopic and genetic data. Especially important has been solid-state NMR data (Zeri et al. 2003) that can give detailed information about the structure of the subunit, although not about the structure of the helical assembly of subunits. The NMR data broadly confirm the X-ray fibre diffraction/molecular model building studies. A model of fd refined against both X-ray fibre diffraction data to 4 Å resolution and solid-state NMR data (PDB entry 2C0X) is shown in Fig. 1a.

Iterative helical real space reconstruction method has been applied to cryoEM images of the fd strain of filamentous phage, and yielded a structural model that is significantly different from models derived by X-ray fibre diffraction and solid-state NMR. Here we examine the differences between the X-ray/NMR model 2C0X (Marvin et al. 2006) and the cryoEM model 2HI5 (Wang et al. 2006). These differences are of two distinct types, the helix symmetry parameters relating one subunit to the next, and the shape of the individual identical subunits; we discuss possible reasons for these differences. We also refine the cryoEM model 2HI5 against the X-ray fibre diffraction data, and show that the cryoEM model can be refined to approximate the X-ray/NMR model 2C0X.

Materials and methods

Preparation of phage and formation of fibres has been described (Marvin 1966; Marvin et al. 1974a; Nave et al. 1981; Welsh et al. 1996). Phage is purified by cycles of low and high speed centrifugation, and the final pellet is taken up in low ionic strength buffer (e.g., 10 mM tris–EDTA, pH 8.0) at a concentration of about 30 mg/ml. A drop of this gel is suspended between the tips of two glass rods and excess water is evaporated under controlled humidity as the fibre forms. The resulting fibres contain as much solvent as is found in many crystals of globular proteins.

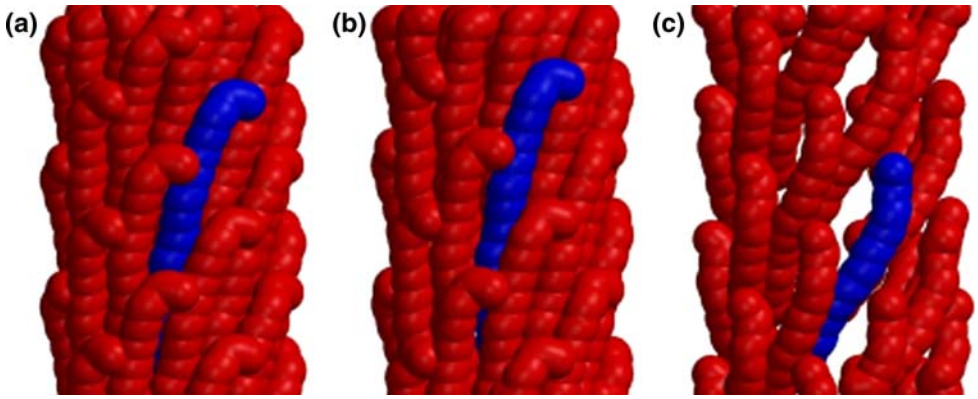

Fig. 1 Models of fd filamentous bacteriophage. In all cases an axial slab about 100 Å long was cut from the array of subunits, and the phage axis is vertical. Each subunit is represented as a twisted ribbon about 10 Å in diameter following the protein backbone. The N-terminus of each subunit is towards the top. Every subunit in the array is colored red except for a single subunit, colored blue to illustrate how each subunit is surrounded by identical symmetry-related subunits. The back clipping plane is adjusted so the back half of the model is deleted (this is not apparent except in **c**, because in **a** and **b** the subunits are so closely packed that one cannot see through the array in front). (**a**) Model 2C0X in the fd^D symmetry, unit height = 16.15 Å, unit twist = 36.0°. (**b**) Model 2C0X slewed into the symmetry of 2HI5, unit height = 17.4 Å, unit twist = 37.4°. (**c**) Model 2HI5. Note the gaps between subunits in this array

Collecting and processing fibre diffraction data has been described (Marvin et al. 1994, 2006; Welsh et al. 1996). We use a single amino acid replacement fd mutant Y21M to avoid the problem of layer line fanning that complicates the fibre diffraction patterns of wild-type fd (Marvin et al. 1994; Welsh et al. 1996), but we find no significant difference between wild-type and Y21M structure at the resolution of the models discussed here. In the cryoEM work it was reported that only about half the images of wild-type fd could be used, but all the images of Y21M (Wang et al. 2006). It is conceivable that this problem may be related to the unusual liquid–crystalline properties of wild-type fd that are avoided with Y21M (Welsh et al. 1996), although the cryoEM experiments presumably use conditions where there is no local packing of phage particles (and therefore no liquid–crystallinity) that might affect the structure of the individual phage particles.

Our diffraction patterns are routinely calibrated by dusting the fibres with powdered crystalline calcite or silicon, giving a powder ring on the diffraction pattern at 3.029 Å (calcite) or 3.136 Å (silicon), and thereby an internal calibration of distance accurate to better than one part in 500.

The subunits of fd in fibres are arranged in groups of five, related by a fivefold rotation axis around the phage helix axis; each such pentamer is related to the next pentamer along the helix by a unit height and a unit twist. Two slightly different forms of fd have been identified (Marvin et al. 1994, 2006) by fibre diffraction: fd^D, with a unit height of 16.15 Å and a unit twist of 36.0°; and fd^C, with a unit height of 16.0 Å and a unit twist of 38.77°. The overall intensity distributions on the diffraction patterns are similar for these two structures, but they can be distinguished by the layer-line splitting (Marvin et al. 1994) on fd^C. "Layer-line splitting" means that diffracted intensity from different diffraction directions that is superimposed because of the symmetry, and therefore not distinguishable on fd^D diffraction patterns is slightly separated, and therefore distinguishable on the fd^C diffraction patterns. In comparing models in different symmetries, the orientation of each subunit must be slewed using Eq. (5) of Marvin (1990), to take account of the fact that the elongated subunit passes between other subunits on higher turns of the bacteriophage helix, and if the phage helix symmetry changes, the orientation of the subunit must also change to avoid steric clashes.

The relative solvent accessible surface areas of residues were calculated essentially as described by Marvin et al. (2006), but using the program AREAIMOL from the CCP4 suite (Collaborative Computational Project, Number 4 1994) to calculate the accessibilities of residues in an isolated subunit and in a subunit surrounded by its nearest-neighbours.

We use the program FX-PLOR (Wang and Stubbs 1993), a modification of X-PLOR (Brünger 1992) for X-ray fibre diffraction data, to refine the 2HI5 cryoEM model essentially as described previously (Marvin et al. 1994, 2006; Welsh et al. 2000). In our discussions we use model 2C0X (refined with respect to both X-ray and NMR data), rather than model 2C0W (refined only with respect to X-ray data); the r.m.s.d between backbone atoms of these two models (Marvin et al. 2006) is only 0.14 Å. Refining against X-ray data requires a full subunit, so we first reorient the X-ray/NMR model 2C0X so that the backbone of residues 7–46 fits the backbone of the corresponding residues of the cryoEM model 2HI5 to a backbone r.m.s.d of 1.7 Å for these residues. We call this reoriented 2C0X model "2HI5-2C0X". We use model 2HI5-2C0X as proxy

for 2HI5 with the missing residues added at the two ends. At the resolution of the cryoEM data (8 Å), these two models are identical for residues 8–46, as tested by superimposing surface displays for the backbones of the two models: the two surface displays sit on top of one another, except for a slight hook at residues 6–8 of model 2HI5. We then refine model 2HI5-2C0X with respect to the X-ray data using simulated annealing from 3,000 to 0 K with rigid-body energy minimization for three segments (residues 1–6, 7–46, 47–50). The three segments were chosen so that the residues missing from 2HI5 were refined separately from those residues present in 2HI5. Initially we omit energy constraints between symmetry-related neighbouring subunits (this is necessary because high initial energy between symmetry-related subunits of the starting model prevents refinement of the starting model) and refine from an initial *R*-value of 0.65 to an *R*-value of 0.38. We then continue the rigid-body simulated annealing, again from 3,000 to 0 K, with energy constraints now included between symmetry-related subunits, to an *R*-value of 0.34, followed by simulated annealing using Powell energy minimization (not rigid-body) to an *R*-value of 0.19. This refinement is not intended to be exhaustive, but only to show that model 2HI5 is moved towards 2C0X by refinement against the X-ray data; however, the coordinates of this refined 2HI5-2C0X low-resolution model described here are available from the authors if desired.

As a simple measure of the fit of calculated to observed NMR data, we compute a normalized difference in the chemical shift $(CS_i^c - CS_i^o)/5$ and a normalized difference in the dipolar coupling $(D_i^c - D_i^o)/0.4$, where i is the residue number, CS_i^c and D_i^c are values calculated as described by Straus et al. (2003), CS_i^o and D_i^o are the observed values (Zeri et al. 2003), 5 ppm is the error in the chemical shift dimension and 0.4 kHz is the error in the dipolar dimension. We add protons to the coordinates using CNS, with the NH distance set to 1.066 Å, as described by Marvin et al. (2006). Then our measure of the fit of calculated to observed solid-state NMR data for residue i is $\Delta_i = (((CS_i^c - CS_i^o)/5)^2 + ((D_i^c - D_i^o)/0.4)^2)^{1/2}$. This is analogous to the penalty function used by others but normalized to put the CS and *D* parameters on a similar scale.

Results and discussion

Helix symmetry

The unit height (meridional spacing) in fd has an average value (Marvin 1966) for hydrated fibres of 16.1 ± 0.1 Å. The unit height remains about the same (16.26 Å) in very wet gels of fd which show no crystal packing between neighbouring virions (Symmons et al. 1995), conditions similar to those used for X-ray fibre diffraction studies of tobacco mosaic virus. Gels of the K48A mutant of fd, that have a lower positive charge density on the inner surface of the protein coat and therefore lower DNA/protein ratio, still have the same unit height in the protein shell (Symmons et al. 1995).

Helix parameters are determined in the IHRSR method by averaging parameters from images of many different helix segments (Egelman 2007). For fd, the signal-to-noise ratio of the images is low, as for all cryoEM images where no stain is used, and it was necessary to average tens of thousands of such images (Wang et al. 2006). Because of heterogeneity and noise in the data, pre-selection of images similar to two initial reconstructions was used to improve the averaging. The resolution of the reconstructions was estimated as 8 Å from the agreement among repeated reconstructions. This approach has the advantage that the chosen datasets are selected for minimum discrepancy from the reconstruction, but has the disadvantage that as a result the resolution estimate may be biased by the selection step. The final two representative reconstructions have similar helix symmetry and similar density distribution at 15 Å resolution (Wang et al. 2006), but their density distribution diverges as the resolution estimate is improved by the selection and averaging process. A complication in the averaging is that subunits within each pentamer as seen by cryoEM might not be related by a precise fivefold rotation axis, and errors may be introduced by the presumption of a perfect pentamer.

Iterative helical real space reconstruction method gives a unit height of 17.4 Å relating successive pentamers (Wang et al. 2006), compared with 16.1 Å from X-ray fibre diffraction. Changes in unit height of about 5% as a function of small changes in humidity or temperature have been identified for Pf1 and fd (Marvin et al. 1974a; Nave et al. 1981; Specthrie et al. 1987; Marvin 1990), so the difference between the X-ray value and the IHRSR value is within the range found experimentally in phage fibres. If the radius of curvature of a curved region of phage is about 1,000 Å as seen in some electron micrographs (Wang et al. 2006), there would be about a 5% difference between the inner and outer circumference of a curved 60 Å wide phage, similar to the observed variation in unit height. We have built the subunit of the fd X-ray/NMR model 2C0X into the helix parameters derived by cryoEM (Fig. 1b), and this model suggests that the phage can be slightly stretched by the cryoEM technique with no significant local distortion of the subunit.

Subunit shape

The significant difference between the shapes of molecular models for single subunits derived from IHRSR on the one

hand and X-ray/NMR on the other hand is more difficult to understand than the difference in helix parameters relating the subunits. The IHRSR subunit molecular model (PDB entry 2HI5) depends not only on the shape of the density distribution (EM Databank entry 1240), but also on the choice of which density to associate with each symmetry lattice point, and the choice of the register between the subunit model and the density. For the X-ray/NMR model 2C0X, diffraction from phage with an iodinated tyrosine on each subunit indicated the radius of the tyrosine (Glucksman et al. 1992; Marvin et al. 1994; Marvin et al. 2006). Accessibility considerations, especially accessibility of sidechains to non-disrupting chemical reagents, further defined the orientation of the subunit around its own axis within the virion, and showed that the N-terminal region of the protein is at the outer surface of the coat and the C-terminal region is at the inner surface, where its basic residues interact with the DNA in the central core (Marvin 1990; Marvin et al. 1994, 2006; Symmons et al. 1995).

Wang et al. (2006) judged by inspection how best to fit a molecular model into the IHRSR reconstruction, in order to derive their PDB entry 2HI5. The radial position of the subunit in the reconstruction was constrained by the radius of the inner surface of the central hole. The radius of this hole appears significantly larger than in the X-ray model. This may indicate that the DNA-associated protein residues in the IHRSR reconstruction are less well ordered than in the fibre diffraction studies, perhaps because of lower ionic strength in the latter (Symmons et al. 1995). Placing the C-terminal residues at the inner surface of the IHRSR envelope means that the full length of the subunit cannot be accommodated and the first six residues have to be omitted despite the larger outer radius of the reconstruction compared with the X-ray/NMR model 2C0X. This larger outer radius of the IHRSR reconstruction might be due to expansion of the structure in the cryoEM experiment or possibly to slight overestimation of the scale of the micrographs, either of which could also explain the somewhat larger unit height of model 2HI5.

The subunits of 2HI5 do not pack well together, leaving nanometre gaps between subunits in the array, which is not an expected structure for a protective virus coat (Fig. 1c). The DNA in the interior of the phage is accessible to deuteration (Wen et al. 1997), but this need not require such large holes in the coat (Hadzi 1988). Hydrophobic residues that are buried in the X-ray/NMR model 2C0X array are accessible to solvent in the 2HI5 array. In particular, NMR experiments show that residues Ile39, Leu41, Phe42 and Phe45 are not accessible to deuteration (Zeri et al. 2003). The relative solvent accessible surface areas of these four residues are all less than 0.06 in the X-ray/NMR model 2C0X array, consistent with the deuteration experiments; but are, respectively, 0.12, 1.0, 0.36 and 0.83 in the cryoEM model 2HI5 array, suggesting a possible inconsistency with the deuteration experiments.

The fit Δ_i between the predicted solid-state NMR pattern of the cryoEM model 2HI5 and the observed NMR data is poor over the whole sequence (Fig. 2). For comparison, Δ_i for the X-ray/NMR model 2C0X (from Fig. 5 of Marvin et al. 2006), also shown in Fig. 2, is much better.

Refinement of the cryoEM model

The fit between the predicted X-ray fibre diffraction pattern of the cryoEM model 2HI5 and the observed X-ray fibre diffraction data is poor (Fig. 3), with an *R*-value of 0.60, and such a large *R*-value is generally taken by crystallographers to indicate an unacceptable model. The 2HI5 cryoEM model was proposed (Wang et al. 2006) as "a starting point for refining the structure" of fd. To explore the possibility of a homometric structure (a model similar to 2HI5 that nevertheless fits the X-ray data), we refined the structure of the cryoEM model 2HI5 against the X-ray fibre diffraction data using simulated annealing as described under "Materials and methods". The model 2HI5-2C0X could be refined to a model with an *R*-value of 0.19 (Fig. 4). In simple terms, the refinement is essentially the same as adding the missing residues to the ends of 2HI5, the red model, and then refining this full subunit against the X-ray data to yield the yellow model, which is close to the X-ray/NMR model 2C0X, the green model. The backbone r.m.s.d between the start and end of this refinement is 6.5 Å, and the final model is not far from the X-ray/NMR model 2C0X (backbone r.m.s.d 1.1 Å). That is, the cryoEM model 2HI5 could be refined to fit the X-ray data, but this involved making large changes to the original 2HI5 coordinates, and yielded a model similar to that determined by X-ray/NMR refinement alone.

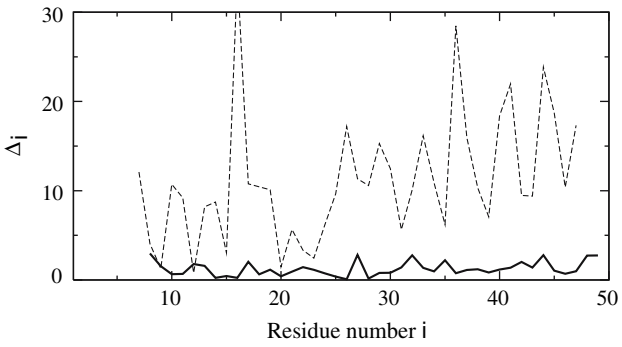

Fig. 2 The fit Δ_i between the calculated solid-state NMR spectrum of fd models and the observed spectrum as a function of residue number *i*. *Solid curves*, Δ_i computed using the calculated spectrum from PDB entry 2C0X (see also Fig. 5 of Marvin et al. 2006); *broken curves*, Δ_i computed using the calculated spectrum from PDB entry 2HI5

Fig. 3 X-ray fibre diffraction pattern of fd filamentous bacteriophage. A single quadrant is shown, with the fibre axis vertical. The outer edge of the diffraction pattern corresponds to about 3 Å spacing. (**a**) Experimentally observed diffraction pattern after background subtraction, mapped from detector space to reciprocal space and quadrant averaged (Fig. 2a of Marvin et al. 2006). (**b**) Calculated simulated diffraction pattern for model 2HI5. The arrow above the first layer line on **b** indicates a region where strong calculated intensity appears at a reciprocal space radius of $R = 0.05$ Å^{-1}, compared with $R = 0.10$ Å^{-1} on the observed diffraction pattern

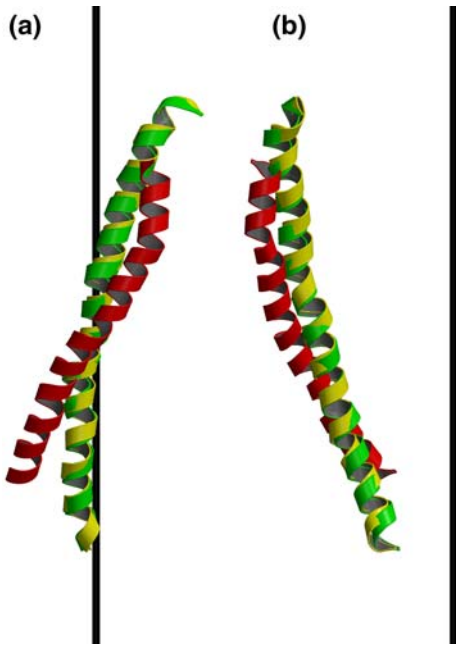

Fig. 4 Refinement of model 2HI5 with respect to X-ray fibre diffraction data. Red, model 2HI5 slewed into fd^{D} symmetry, before refinement; *green*, model 2C0X; *yellow*, model 2HI5-2C0X after refinement against the X-ray data. *Vertical line* is the bacteriophage helix axis. The N-termini of the subunits are towards the top in all cases. (**a**) View along a radius of the cylindrical-polar coordinate system towards the helix axis from outside the bacteriophage. (**b**) View perpendicular to **a**

Filamentous phage in solution is well-known to be flexible, which means that in solution there cannot be a constant rigid relationship between subunits throughout the phage. Model coordinates for two structural forms of fd and two forms of the structurally similar but genetically unrelated strain Pf1 have been deposited (Marvin 1998; Marvin et al. 2006), and these different models illustrate the extent of changes that the structures may undergo as they flex in solution. Helix parameters and the subunit shape must both vary to some extent along the length of the phage in solution. But it is difficult to see any structural explanation for large differences in subunit shape between models derived using the two experimental conditions, cryoEM and X-ray fibre diffraction. It might be proposed that the cryoEM and X-ray fibre diffraction results differ because "dried" fibres are used in fibre diffraction (Wang et al. 2006), but this suggestion reflects a misunderstanding of the experimental method for making fibres, which does not involve a drying step. Even fibres of fd that have been deliberately dried far below the solvent content usually used for fibre diffraction experiments (to enable calculation of the minimum unit cell volume) contain 11% by weight water (Nave et al. 1981). X-ray diffraction shows little difference in structure of Pf1 phage between fibres and oriented solutions (Specthrie et al. 1987). Magic-angle spinning solid-state NMR experiments on unoriented samples of Pf1 show a subunit structure similar to that found by fibre diffraction, with no evidence for more than one subunit conformation in the sample (Goldbourt et al. 2007). It would be interesting if the cryoEM conditions cause the phage length to increase slightly relative to the length in liquid crystals, but none of the experimental evidence leads one to postulate a major change in subunit structure.

There is no evidence in the X-ray or NMR data that model 2HI5 or any similar model provides a reasonable representation of the structure of the fd subunit in fibres. If 2HI5 is used as a starting point for refinement against the X-ray data, it can indeed be refined, and the result is a model close to the X-ray/NMR model 2C0X. If no other information were available, cryoEM might be a useful first step in the analysis of fd structure. But the idea that the structure of intact phage fd in solution is substantially different from that in fibres does not seem possible. Virus coats must be locally stable, not subject to major distortion by mild environmental conditions, and indeed fd infectivity is known to be stable up to a temperature of 80° C, to pH between pH 2.5 and 10.5, and to drying under vacuum.

One possible flaw in the IHRSR method is that the subunits within each pentamer in the cryoEM images are presumed to be related by a precise fivefold rotation axis. But there may be perturbations in the relationship between unit height, unit twist and rotation axis, as discussed in early attempts to determine the fd symmetry in fibres (Marvin et al. 1974b). Errors in the reconstruction would be introduced if such perturbations are present in the images but not correctly treated in the averaging. This question is not addressed by Wang et al. (2006). We find that the X-ray/NMR model 2C0X remains the better representation of fd filamentous bacteriophage.

Acknowledgments We are grateful to Professors E.H. Egelman and G.J. Thomas, Jr for valuable discussions and for sending us the coordinates of PDB entry 2HI5 before release. WRPS would like to acknowledge support from the Canada Foundation for Innovation. SKS would like to acknowledge support from the Natural Sciences and Engineering Research Council of Canada (University Faculty Award and Discovery Grant) and from the University of British Columbia. MFS is an Oppenheimer Research Fellow.

References

Banner DW, Nave C, Marvin DA (1981) Structure of the protein and DNA in fd filamentous bacterial virus. Nature 289:814–816

Brünger AT (1992) X-PLOR Version 3.1, Yale University Press, New Haven

Bryan RK, Bansal M, Folkhard W, Nave C, Marvin DA (1983) Maximum-entropy calculation of the electron density at 4 Å resolution of Pf1 filamentous bacteriophage. Proc Natl Acad Sci USA 80:4728–4731

Collaborative Computational Project, Number 4 (1994) The CCP4 suite: programs for protein Crystallography. Acta Crystallogr Sect D 50:760–763

Egelman EH (2000) A robust algorithm for the reconstruction of helical filaments using single-particle methods. Ultramicroscopy 85:225–234

Egelman EH (2007) The iterative helical real space reconstruction method: Surmounting the problems posed by real polymers. J Struct Biol 157:83–94

Glucksman MJ, Bhattacharjee S, Makowski L (1992) Three-dimensional structure of a cloning vector. X-ray diffraction studies of filamentous bacteriophage M13 at 7 Å resolution. J Mol Biol 226:455–470

Goldbourt A, Gross BJ, Day LA, McDermott AE (2007) Filamentous phage studied by magic-angle spinning NMR: resonance assignment and secondary structure of the coat protein in Pf1. J Am Chem Soc 129:2338–2344

Gonzalez A, Nave C, Marvin DA (1995) Pf1 filamentous bacteriophage: Refinement of a molecular model by simulated annealing using 3.3 Å resolution X-ray fibre diffraction data. Acta Crystallogr Sect D 51:792–804

Hadzi D (1988) Proton transfers in biological mechanisms. J Mol Struct 177:1–21

Marvin DA (1966) X-ray diffraction and electron microscope studies on the structure of the small filamentous bacteriophage fd. J Mol Biol 15:8–17

Marvin DA (1990) Model-building studies of *Inovirus*: genetic variations on a geometric theme. Int J Biol Macromol 12:125–138

Marvin DA (1998) Filamentous phage structure, infection and assembly. Curr Opin Struct Biol 8:150–158

Marvin DA, Wachtel EJ (1976) Structure and assembly of filamentous bacterial viruses. Philos Trans R Soc Lond Series B 276:81–98

Marvin DA, Wiseman RL, Wachtel EJ (1974a) Filamentous bacterial viruses. XI. Molecular architecture of the class II (Pf1, Xf) virion. J Mol Biol 82:121–138

Marvin DA, Pigram WJ, Wiseman RL, Wachtel EJ, Marvin FJ (1974b) Filamentous bacterial viruses. XII. Molecular architecture of the class I (fd, If1, IKe) virion. J Mol Biol 88:581–600

Marvin DA, Bryan RK, Nave C (1987) Pf1 *Inovirus*: Electron density distribution calculated by a maximum entropy algorithm from native fibre diffraction data to 3 Å resolution and single isomorphous replacement data to 5 Å resolution. J Mol Biol 193:315–343

Marvin DA, Hale RD, Nave C, Helmer-Citterich M (1994) Molecular models and structural comparisons of native and mutant class I filamentous bacteriophages Ff (fd, f1, M13), If1 and IKe. J Mol Biol 235:260–286

Marvin DA, Welsh LC, Symmons MF, Scott WRP, Straus SK (2006) Molecular structure of fd (f1, M13) filamentous bacteriophage refined with respect to X-ray fibre diffraction and solid-state NMR data supports specific models of phage assembly at the bacterial membrane. J Mol Biol 355:294–309

Nave C, Brown RS, Fowler AG, Ladner JE, Marvin DA, Provencher SW, Tsugita A, Armstrong J, Perham RN (1981) Pf1 filamentous bacterial virus. X-ray fibre diffraction analysis of two heavy-atom derivatives. J Mol Biol 149:675–707

Russel M, Model P (2006) Filamentous phage. In: Calendar RL (ed) The bacteriophages, 2nd edn. Oxford University Press, USA, pp 146–160

Specthrie L, Greenberg J, Glucksman MJ, Diaz J, Makowski L (1987) Structural responsiveness of filamentous bacteriophage Pf1: Comparison of virion structure in fibers and solution. Biophys J 52:199–214

Straus SK, Scott WRP, Watts A (2003) Assessing the effects of time and spatial averaging in ^{15}N chemical shift/^{15}N–^{1}H dipolar correlation solid state NMR experiments. J Biomol NMR 26:283–295

Symmons MF, Welsh LC, Nave C, Marvin DA, Perham RN (1995) Matching electrostatic charge between DNA and coat protein in filamentous bacteriophage. Fibre diffraction of charge-deletion mutants. J Mol Biol 245:86–91

Thiriot DS, Nevzorov AA, Zagyanskiy L, Wu CH, Opella SJ (2004) Structure of the coat protein in Pf1 bacteriophage determined by solid-state NMR spectroscopy. J Mol Biol 341:869–879

Wang H, Stubbs G (1993) Molecular dynamics in refinement against fiber diffraction data. Acta Crystallogr Sect A 49:504–513

Wang YA, Yu X, Overman S, Tsuboi M, Thomas GJ Jr, Egelman EH (2006) The structure of a filamentous bacteriophage. J Mol Biol 361:209–215

Webster RE (2001) Filamentous phage biology. In: Barbas CF III, Burton DR, Scott JK Silverman GJ (eds) Phage display: a laboratory manual. Cold Spring Harbor Laboratory Press, Cold Spring Harbor, pp 1.1–1.37

Welsh LC, Symmons MF, Nave C, Perham RN, Marseglia EA, Marvin DA (1996) Evidence for tilted smectic liquid crystalline packing of fd *Inovirus* from X-ray fiber diffraction. Macromolecules 29:7075–7083

Welsh LC, Symmons MF, Marvin DA (2000) The molecular structure and structural transition of the α-helical capsid in filamentous bacteriophage Pf1. Acta Crystallogr Sect D 56:137–150

Wen ZQ, Overman SA, Thomas GJ Jr (1997) Structure and interactions of the single-stranded DNA genome of filamentous virus fd: Investigation by ultraviolet resonance Raman spectroscopy. Biochemistry 36:7810–7820

Zeri AC, Mesleh MF, Nevzorov AA, Opella SJ (2003) Structure of the coat protein in fd filamentous bacteriophage particles determined by solid-state NMR spectroscopy. Proc Natl Acad Sci USA 100:6458–6463